

Non-Arrhenius stretched exponential dielectric relaxation in antiferromagnetic TiBO_3 single crystals

A. A. Bokov, M. Mahesh Kumar, Z. Xu, and Z.-G. Ye*

Department of Chemistry, Simon Fraser University, Burnaby, BC, Canada 5A 1S6

(Received 13 April 2001; published 13 November 2001)

Dielectric spectra of TiBO_3 single crystals, grown by the chemical vapor transport technique, have been studied at temperatures between 40 and 200 °C and frequencies from 100 Hz to 1 MHz. The shape of the spectra is well parameterized in terms of the temperature-independent Kohlrausch-Williams-Watts (stretched exponential) form, modified with the superimposed low-frequency dispersion and dc component. A deviation of the relaxation time from the Arrhenius law has been observed, which cannot be fitted into the known formulas. This deviation is phenomenologically explained by the screening effect. A formula has been proposed to describe such a complex dielectric relaxation behavior that is expected to exist in many more materials.

DOI: 10.1103/PhysRevB.64.224101

PACS number(s): 77.22.Gm, 77.22.Ch, 77.84.-s

I. INTRODUCTION

The compounds of $M\text{BO}_3$ family, where M is a trivalent transition-metal ion, crystallize into a calcite-type structure.¹ FeBO_3 has been the most studied compound of this family due to the interest generated by its magnetic properties. It is an antiferromagnet with a Néel temperature (T_N) around 348 K, associated with a weak ferromagnetism above room temperature.² Such a relatively high T_N , which is unusual for oxide systems, facilitates the investigation of critical phenomena. Added to this is the crystal transparency in the visible region right up to the Néel temperature, which makes it a potential candidate for high-speed magneto-optic applications. Recently, intensive investigations have been carried out on the electronic structure and magnetic properties of FeBO_3 .³⁻⁷

So far not a single study of the physical properties of the titanium borate TiBO_3 has been reported. This is mainly due to the difficulties encountered in synthesizing TiBO_3 crystals, which requires the stabilization of Ti^{3+} valence state with d^1 configuration. Recently,⁸ we have successfully grown the single crystals of TiBO_3 with controlled trivalent state of Ti^{3+} , using a specially designed chemical vapor transport technique.⁹ The availability of single crystals has allowed us to investigate the dielectric, electric, and magnetic properties of TiBO_3 . The magnetic measurements by superconducting quantum interference device show that TiBO_3 behaves as an antiferromagnet with a magnetic phase transition at $T_N = 23$ K.¹⁰

This paper reports the results of the first dielectric spectroscopic study of TiBO_3 single crystals. The dielectric response of TiBO_3 is found to exhibit frequency dispersion and relaxation, which can be described phenomenologically using a modified stretched exponential form.

II. THEORETICAL APPROACH

The dielectric relaxation in condensed systems can often be described by the Kohlrausch-Williams-Watts (KWW) function (or the “stretched exponential” function)¹¹⁻¹³

$$\Phi(t) = \exp[-(t/\tau_{\text{KWW}})^\beta], \quad (1)$$

and/or by the empirical Havriliak-Negami (HN) function

$$\varepsilon^*(\omega) = \varepsilon_\infty + \chi_{\text{HN}}^* = \varepsilon_\infty + \frac{\varepsilon_s - \varepsilon_\infty}{[1 + (i\omega\tau_{\text{HN}})^\alpha]^\gamma}. \quad (2)$$

In the above expressions, χ_{HN} stands for complex susceptibility representing relaxation process, $\omega = 2\pi f$ is the angular frequency, ε_∞ represents the asymptotical value or the permittivity at high frequencies, ε_s is the value of the opposite limit, τ_{NH} and τ_{KWW} stand for relaxation time (which, in general, is not equal to the reciprocal frequency of the loss peak, ω_m), α , β , and γ are parameters determining the spectral shape ($0 < \alpha, \beta, \alpha\gamma \leq 1$).

The KWW function deals with the data in time domain, while the HN expression is used in the frequency domain (the well-known Cole-Cole and Cole-Davidson expressions are the limiting forms of the HN function with $\gamma=1$ and $\alpha=1$, respectively). The KWW law (1) was found to apply not only to dielectrics, but also to other forms of relaxation, including mechanical, enthalpic, light scattering, nuclear magnetic resonance (NMR), magnetic relaxation, chemical reactions, luminescence decay, quasi-elastic neutron scattering, etc. This law is not just an empirical expression, but has a profound theoretical significance.¹² In particular, the rigorous mathematical investigation on the basis of theory of stochastic phenomena showed that only certain solutions of the relaxation function are possible and this function has the KWW form (1).¹⁴ This conclusion is valid independently of any microscopic physical model; it is dictated exclusively by the stochastic nature of the relaxation process. To obtain the more complex HN relaxation form, it is necessary to introduce in the stochastic analysis the concept of clusters composed of the relaxing entities having common motions due to mutual interactions.¹⁵ On the other hand, the consideration in the frame of percolation theory revealed a direct connection between the KWW relaxation and the fractal nature of material. The space fractal structure necessarily leads to the stretched exponential relaxation, and the inverse relation was

suggested to hold, namely, when a system is observed to relax in a stretched exponential way, it is the signature of the fractal morphology.¹⁵

To determine if the frequency dependence of the permittivity in a particular material corresponds to the KWW-type relaxation, one can transform the KWW function into the frequency domain by means of Fourier transformation of its time derivative,

$$\begin{aligned}\varepsilon^*(\omega) &= \varepsilon_\infty + \chi_{\text{KWW}}^* \\ &= \varepsilon_\infty + (\varepsilon_s - \varepsilon_\infty) \int_0^\infty (-d\Phi/dt) \exp(-i\omega t) dt, \quad (3)\end{aligned}$$

and use the result to fit the experimental $\varepsilon^*(\omega)$ data. It is known that the Fourier transform (3) does not coincide exactly with the HN function (which is usually employed for fitting in the frequency domain). Thus, one can expect the existence of an approximate correspondence between Eqs. (2) and (3). Such a correspondence was established after a great deal of work,^{16,17} but it appears to be valid only in the vicinity of the loss-peak frequency (note that any Fourier transform of KWW function into frequency domain can be approximated by a HN function, but not vice versa). On the other hand, there exists a rigorous way to discriminate between HN and KWW functions in the frequency domain. At frequencies much lower than the loss-peak frequency, the HN function follows the relation $\varepsilon'' \propto f^\alpha$, but the KWW form gives the relation $\varepsilon'' \propto f$ (which is valid only in the Cole-Davidson limit of the HN function).

The analysis of this behavior by Hill^{18,19} based on the literature data revealed that among a hundred dipolar materials, only ten show a low-frequency slope of the loss peak, which is compatible with KWW formula. It is important to mention for further discussion that all these ten examples refer to the dispersion observed at high frequencies. Thus, the question arises as to why the KWW law, which is believed to be a fundamental one in the time domain, seems to work so scarcely in the frequency domain. By the analysis of the dielectric properties of TiBO_3 , we attempt to find an answer to this question.

We will show that TiBO_3 is an example of the materials in which the loss peak can be well fitted to the HN function, while the KWW form cannot be used satisfactorily. Nevertheless, the real spectral shape of the relaxation process is of KWW type, but the dielectric spectrum is distorted by the superimposed contributions from other processes. This situation is expected to be common to many more materials. We have also found a deviation from the Arrhenius law $\tau = \tau_0 \exp(E/kT)$ for the temperature dependence of the relaxation time in TiBO_3 crystals. Such deviations in other materials are usually accompanied by a temperature-induced change in the shape of the loss peak, which remains unchanged in the case of TiBO_3 .

III. EXPERIMENT

Single crystals of TiBO_3 were grown via chemical vapor transport taking place in a sealed quartz tube at 950 °C for 120 h. The grown crystals show a dark brown color with

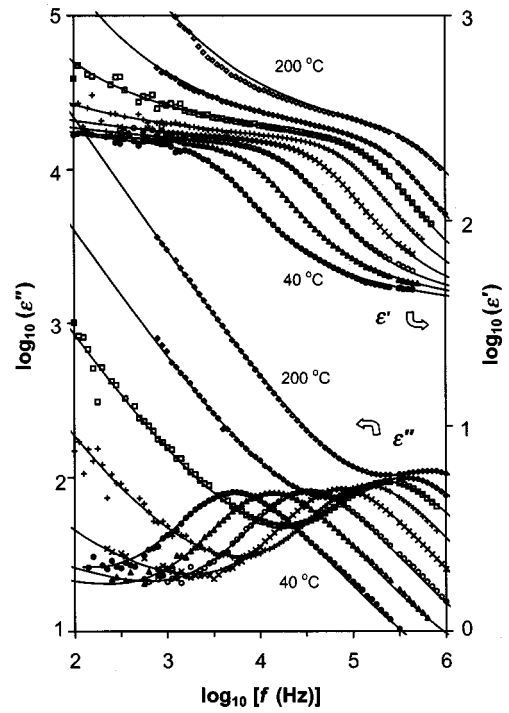


FIG. 1. Frequency dependences of the real (upper set of curves) and the imaginary parts (lower set of curves) of dielectric permittivity of a TiBO_3 crystal measured at different temperatures (from left to right): $T=40, 60, 80, 100, 120, 140, 160,$ and 200 °C. The solid lines represent the fits to Eq. (4) with the terms calculated by Eqs. (3), (5)–(7).

hexagonal platelet or polyhedral morphology and a typical size of $0.5 \times 0.5 \times 0.2$ mm³. The two parallel (001) faces of the crystals were painted with silver paste and a gold wire was attached to each of them. The electrode connections were made after drying at 80 °C for 2 h.

Dielectric spectroscopic measurements were performed by means of a computer-controlled Solartron-1260 Impedance Analyzer/Solartron 1296 Dielectric Interface system, in the frequency range of 100 Hz to 1 MHz and in the temperature interval between 40 and 200 °C. To avoid any possible oxidation of Ti^{3+} ions, the sample was heated in a silicon oil bath, the temperature of which was sensed by a Cr-Al thermocouple and controlled by an Omega CN3000 temperature controller.

IV. RESULTS AND ANALYSIS

The experimental data on the frequency dependences of real (ε') and imaginary (ε'') parts of relative permittivity at various temperatures are presented in Fig. 1. The plots show two visible relaxation processes. The first one manifests itself as a Debye-like peak in $\varepsilon''(f)$ with a corresponding drop in $\varepsilon'(f)$. The $\varepsilon''(f)$ peak [or the $\varepsilon'(f)$ drop] observed at about 5 kHz for 40 °C shifts to higher frequencies with increasing temperature. The variation of the frequency of ε'' maximum (f_m) as a function of reciprocal temperature exhibits a nonlinear dependence, indicating a non-Arrhenius behavior, as shown in Fig. 2.

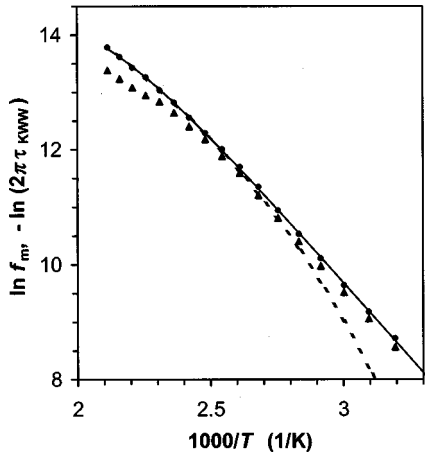


FIG. 2. Dependences upon reciprocal temperature of (i) the logarithm of the reciprocal relaxation time (τ_{KWW}) obtained from the fitting of dielectric spectra to Eq. (4) (filled circles), and (ii) the logarithm of the loss-peak frequency (f_m , triangles). Solid and broken lines represent the fits of τ_{KWW} data to Eq. (8) and to the Vogel-Fulcher law, respectively, in the high-temperature range (130–200 °C), and the extrapolations of the fitted curves to lower temperatures.

The second relaxation process appears as a steep rise in the values of $\varepsilon'(f)$ and $\varepsilon''(f)$ in the low-frequency range at high temperatures. In the frequency range where this process dominates, it is possible to describe the loss curves by the fractional power law $\varepsilon'' \propto f^{n-1}$, with a practically temperature-independent parameter value of $n \approx 0.15$. Such a behavior of dielectric permittivity is known as “universal law.”¹¹ The closeness of n values to zero and the extremely high value of $\varepsilon'' (> 10^3)$ allow us to refer the frequency dependence of permittivities in TiBO_3 to the category of low-frequency dispersion (LFD). This kind of dispersion was widely observed in different materials and is usually attributed to the polarization of slowly mobile electronic or ionic charge carriers.¹¹ In the case of LFD, the real part of permittivity ε' also increases with decreasing frequency according to the fractional power law $\varepsilon' \propto f^{n-1}$ with the same parameter n (there is an apparent difference between the LFD and the dc-related loss at which ε' remains frequency independent). Due to the closeness of the n value to zero, the values of ε' at LFD should be much smaller than ε'' at the same frequency [see Eq. (6)], so that the pure power law for ε' cannot be observed as a result of overlap with the dominant contributions from the first (high-frequency) polarization process. Nevertheless, the corresponding rise of ε' with decreasing frequency is clearly visible. At lower frequencies or higher temperatures, the validity of the power law for ε' can also be expected.

We have found that the low-temperature part of experimental data can be normalized into a single-valued curve by plotting the frequency dependences of loss in the coordinates of $\log_{10}(f/f_m)$ vs $\varepsilon''(f)/\varepsilon''(f_m)$ for each temperature. The results of normalization are shown in Fig. 3. It can be seen that all the low-temperature curves, except for the very low-frequency ones, collapse onto a single curve. But the normalization is perturbed for the high-temperature part of spec-

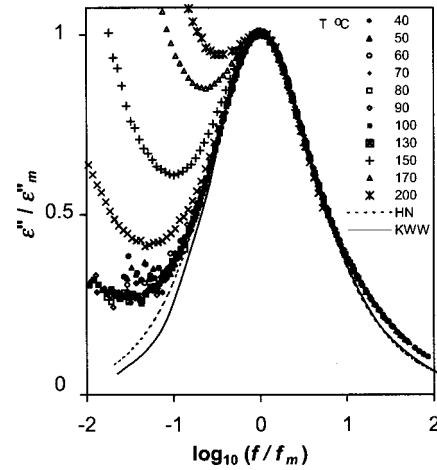


FIG. 3. Normalized plots of the dielectric losses against frequency at several temperatures (f_m represents the loss-peak frequency, ε''_m the loss-peak amplitude). Dashed and solid lines represent the fit to the Havriliak-Negami function [Eq. (2)] and to the Kohlrausch-Williams-Watts form [Eq. (3)], respectively, obtained with the following values of parameters: $\alpha = 0.87$, $\gamma = 0.89$, and $\beta = 0.77$.

trum, where the experimental data deviate from the master curve in the whole frequency range. Such a deviation is clearly due to the overlapping LFD that appears at high temperatures. The reasons for the small deviations observed at low frequencies and low temperatures will become clear in the following discussion. The analogous master curve can also be constructed for the real part of permittivity (not shown).

The existence of a master curve indicates that the spectral shape of relaxation process does not change with temperature. In order to describe this shape analytically, we have tested both HN and KWW formulas. In the course of fitting to the imaginary parts of Eq. (2) or (3), the values of α , γ (or β), and τ_{NH} (or τ_{KWW}) were considered as free parameters that were changed independently to obtain the best results. The value of integral in Eq. (3) was calculated numerically. It appeared impossible to fit experimental data in the whole frequency range reasonably well, and the successful fitting was performed in the vicinity of $\varepsilon''(f)$ maximum only (Fig. 3). It is evident that the HN function fits in the low-frequency range much better than does the KWW form, but both of them fail at very low and very high frequencies.

To explain this failure, we recall the fact that the LFD is accompanied, as a rule, by a high-frequency tail, which follows the “universal law,” $\varepsilon' \propto \varepsilon'' \propto f^{n-1}$, but with an n value much larger than that at low frequencies (usually $n > 0.6$) and with moderate values of loss (usually $\varepsilon'' < 10$ in the radio frequency range).¹¹ This tail spreads over many decades of frequency and due to a large n , appears as a background that is slightly dependent on frequency. It can be considered as the result of a separate relaxation process. We will show below that taking into account this mechanism, one can describe the dielectric spectrum of TiBO_3 perfectly.

The final fitting was performed using the following equation:

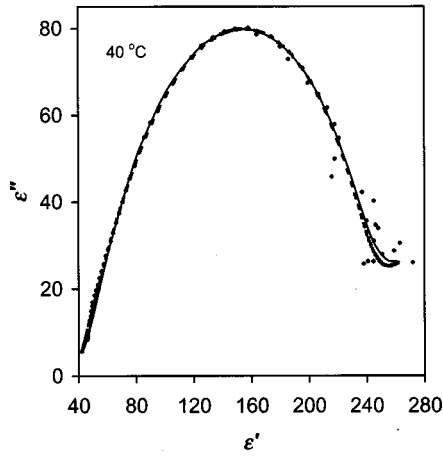


FIG. 4. Complex plane plot of the losses against the real permittivity at 40 °C. Solid line represents the fit to Eq. (4). Broken line is the fit to Eq. (4) in which the susceptibility χ_{KWW}^* is substituted by χ_{HN}^* . The best-fit values of α , γ , A_1 , n_1 , ε_∞ , and $(\varepsilon_s - \varepsilon_\infty)$ are equal to 0.016, 0.668, 79, 0.73, 36, and 176, respectively.

$$\varepsilon^*(\omega) = \varepsilon_\infty + \chi_1^* + \chi_2^* + \chi_{\text{KWW}}^* - i \frac{\sigma}{\omega \varepsilon_0}, \quad (4)$$

where the real value of ε_∞ can be considered related to all “fast” processes, including nonrelaxational electronic and lattice polarizations and any other polarizations with the relaxation regime lying in a frequency range much higher than the measurement frequencies, the susceptibility χ_{KWW}^* is expressed by Eq. (3), ε_0 is the permittivity of free space, and the last term refers to the contribution from dc conductivity σ (the high-temperature data cannot be fitted reasonably well without taking into account the dc-related losses). The values of $\chi_i^* = \chi_i' - i\chi_i''$ stand for the LFD ($i=1$) and for the high-frequency low-loss “universal” component ($i=2$). The imaginary parts are expressed in the conventional way,¹¹

$$\chi_i'' = A_i f^{n_i - 1}. \quad (5)$$

The real parts are considered as the Kramers-Kronig transforms of the imaginary ones:

$$\chi_i' = \chi_i'' \tan(n_i \pi / 2). \quad (6)$$

The fitting procedure was divided into several steps. In all the cases, the real and imaginary parts of the spectra were fitted simultaneously (with the same parameters) for a given temperature. Since the LFD and the dc conductivity at low temperatures are expected to be negligible, the initial fitting was performed at 40 °C with $\chi_1'' = \chi_1' = \sigma = 0$. The parameters ε_∞ , ε_s , A_2 , n_2 , β , and τ_{KWW} were considered as independent variables. The best fits were obtained with $\beta=0.83$, which are shown by solid lines in Fig. 1 as the frequency dependences of ε' and ε'' , and in Fig. 4 in a complex plane. As shown above, the shape of the KWW relaxation peak (which is determined by β) is temperature-independent. Thus, the value of β was fixed to be 0.83 in the further fitting.

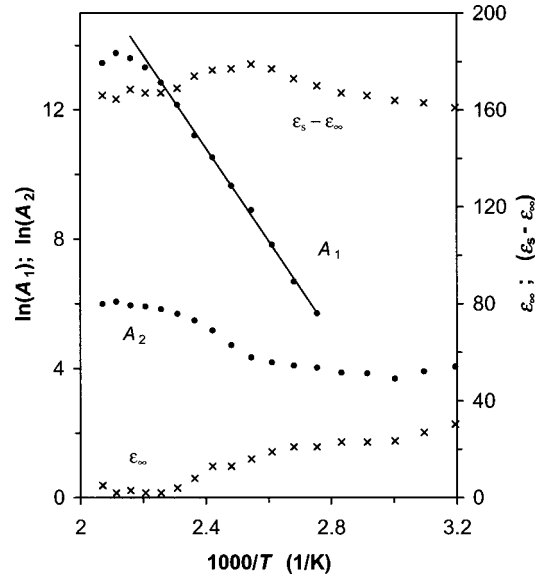


FIG. 5. Dependences upon reciprocal temperature of the parameters A_1 , A_2 , ε_∞ , and $(\varepsilon_s - \varepsilon_\infty)$ obtained from the fitting of dielectric spectra to Eq. (4).

The second step dealt with the fitting of the two high-temperature points (150 and 210 °C) in succession with the variables ε_∞ , ε_s , A_1 , n_1 , A_2 , n_2 , τ_{KWW} , and σ (with β fixed). The best-fit values of σ obtained at these two temperatures were used to calculate the activation energy of dc conduction (E_σ) and the preexponential factor σ_0 using the standard formula

$$\sigma = \sigma_0 \exp(-E_\sigma / kT). \quad (7)$$

The values of E_σ and σ_0 were found to be 1.2 eV and $6 \times 10^7 \Omega^{-1} \text{m}^{-1}$, respectively. Note that, because of a narrow temperature interval used in the fitting, the E_σ value gives the magnitude of the activation energy only.

Fittings at all other temperatures were performed by varying ε_∞ , ε_s , A_1 , n_1 , A_2 , n_2 , and τ_{KWW} , with the value of β fixed at 0.83 and the value of σ calculated for each temperature from Eq. (7) using the above-mentioned values of E_σ and σ_0 . The temperature dependences of the best-fit values of the parameters are presented in Figs. 2 and 5. The values of exponents are found to be practically temperature independent ($n_1=0.81-0.85$; $n_2=0.144$), which is consistent with the known fact that for a given material, n is usually constant or depends on temperature only weakly.¹¹

An excellent agreement between the calculated and the experimental frequency dependences of ε' and ε'' has been obtained for all temperatures. Figure 1 shows such a consistency for selected temperatures, and Fig. 4 represents the dependence in the complex plane for 40 °C.

Fairly good fitting results can be obtained using the HN function instead of the KWW one in Eq. (4). This is not surprising in view of the above-mentioned correlation between them. The example of such fitting is given in Fig. 4. The linear dependence of $\ln A_1$ vs $1/T$, as represented by the solid line in Fig. 5, points to a thermally activated nature of the relaxation responsible for LFD (with $E_a = 1.24$ eV).

It is found that the Arrhenius law is not valid for the temperature dependence of relaxation time τ_{KWW} . Like in the case of f_m , the function $\ln(1/\tau_{\text{KWW}})$ vs $1/T$ shows a curvature, which is clearly visible at high temperatures and becomes less significant (but still remains) with decreasing temperature (Fig. 2). In other words, the mechanism of relaxation causing the violation of the Arrhenius law becomes more and more pronounced with increasing temperature.

The non-Arrhenius behavior of dielectric relaxation is a characteristic of the systems having significant disorder in structure and (or) phase transformations, such as the glass-forming liquids and polymers,^{20,21} orientation glasses,²² and relaxor ferroelectrics.²³ In those cases, the well-known Vogel-Fulcher (VF) relation $\tau = \tau_0 \exp[E_{\text{VF}}/k(T - T_0)]$ is often employed to describe the temperature dependence of the relaxation time τ . When the system approaches the temperature T_0 , the dielectric properties are usually characterized by a broadening of the relaxation spectrum. In particular, in materials forming a glassy state,²¹ the KWW exponent typically depends on temperature as $\beta \sim (T - T_0)$. In TiBO_3 , however, we have observed a dielectric process whose relaxation time significantly deviates from the Arrhenius behavior, while the spectral shape remains unchanged at the same time.

To investigate the applicability of the Vogel-Fulcher relation, we tried to fit the experimental data by using least squares method in the whole temperature range (40–200 °C) as well as in different temperature intervals. The quality of fitting was assessed by the coefficient χ^2 , which is the commonly accepted measure for the quality of a fit. Fitting in the whole temperature range gives rise to the following parameters: $\tau_0 = 2 \times 10^{-10}$ s, $E_{\text{VF}} = 0.2$ eV, $T_0 = 112$ K, and $\chi^2 = 2.4 \times 10^{-3}$. But when fitting was made in narrower temperature intervals, the best-fit parameters are considerably different. The broken line in Fig. 2 shows, as an example, the results of fitting to the VF law in the high-temperature range (130–200 °C), with the best-fit parameters $\tau_0 = 3 \times 10^{-9}$ s, $E_{\text{VF}} = 0.09$ eV, and $T_0 = 214$ K. More significantly, the extrapolation of the VF fitting with the same parameters to the low-temperature range (the broken line) deviates radically from the experimental points. The value of χ^2 , calculated for the whole temperature range by using extrapolation, becomes very large, e.g., $\chi^2 = 0.46$ for the example shown in Fig. 2. Thus, we can conclude that the VF law cannot satisfactorily describe the experimental data. Fittings to some other known theoretical formulas, such as those presented by Eqs. (3) in the review by Rault,²¹ and the relation from the Dissado and Hill theory [see Eq. (8.10) in Ref. 11], were also tried, but the results are not better.

Note that the VF relation coincides with the Arrhenius law at very high temperatures, $T \gg T_0$. It can be formally presented as the Arrhenius law in which the activation energy progressively increases with the lowering of temperature (the VF relation could be derived by means of the theoretical explanation of such an increase²⁴). The situation of TiBO_3 is the inverse: we observe an almost Arrhenius $\tau_{\text{KWW}}(T)$ dependence at low temperatures and a deviation from that dependence at high temperatures, which is believed to result from the increase in activation energy with increasing temperature. We suggest that such an increase in activation en-

ergy is caused by screening effects. It was theoretically argued by Jonscher^{11,25} that all polarizing species (dipoles or hopping charges) in a material, irrespective of their nature, are subjected to the screening by the neighboring polarizing species of the same nature. It was shown that this kind of screening broadens the dielectric spectrum. Evidently, the moving charges other than the considered polarizing species (including free carriers) can also take part in the screening. We believe that in TiBO_3 , the screening by thermally activated carriers gives rise to the change of the activation energy of polarization and consequently leads to the violation of the Arrhenius law.

To discuss this effect in more detail, it is necessary to note that every single dipole contributing to the polarization process in a solid can be considered as a charge, which may hop (due to thermal excitation) between two (or more) localized potential wells.²² The height of the potential barrier between wells (E) determines the frequency of hopping, and consequently, the position of the loss peak (i.e., the relaxation time of the process). The charge localized in the well attracts oppositely charged particles (including free carriers) from the neighborhood. Such a screening results in a deepening of the well, a rise of activation energy, and consequently an increase of relaxation time. Thus, the activation energy becomes a function of the density of screening particles $E = E(n)$. Expanding this function into a series and taking the first approximation in the linear term, we can write $E(n) = E_0 + an$. Assuming the usual temperature dependence $n \propto \exp(-E_b/kT)$ for the density of screening charges, we obtain a modified Arrhenius law:

$$\ln \tau = \ln \tau_0 + \frac{E_0 + b \exp\left(-\frac{E_b}{kT}\right)}{kT}, \quad (8)$$

where E_0 refers to the activation energy at low temperatures where the screening by carriers under consideration is negligible.

The least square fitting of the above-determined relaxation time τ_{KWW} to Eq. (8) gives rise to very satisfactory results with the parameters $\tau_0 = 1.3 \times 10^{-12}$ s, $E_0 = 0.46$ eV, $b = 134$ eV, and $E_b = 0.35$ eV, and the coefficient $\chi^2 = 6.7 \times 10^{-4}$ (which is significantly better than the VF fitting). Independent fittings within narrower temperature intervals lead to almost the same best-fit parameters. Moreover, the dependences so extrapolated can very well describe the experimental data in the whole temperature range. The solid line in Fig. 2 was obtained by fitting the experimental data in the high-temperature range (130–200 °C) and subsequently extrapolating into low-temperature range. The value of χ^2 ($= 1.3 \times 10^{-3}$), calculated for this extrapolated curve using the experimental data from the whole temperature range (40–200 °C), is smaller than that obtained from the VF fitting. All this confirms that Eq. (8) is the right formula to describe the observed dielectric relaxation behavior in TiBO_3 .

V. DISCUSSION AND CONCLUSIONS

TiBO₃ shows an example of materials whose relaxation spectrum can be much better described in the frequency domain by the single HN function than by the single KWW function, as shown in Fig. 3. Nevertheless, the real spectral shape of the relaxation process, responsible for the loss peak, may be of KWW type. But it is distorted by the superimposed contributions of “universal” response [Eqs. (5) & (6)], which is effective in a very wide range of frequencies. The KWW function cannot describe this superposition even approximately, while the HN function can do it because of its higher versatility related to the presence of two shape parameters, α and γ . We have recently reported an analogous example of such a behavior in relaxor ferroelectric Pb(Mg_{1/3}Nb_{2/3})O₃–PbTiO₃ solid solution system.²⁶

The “universal” dispersion described by Eqs. (5) and (6) with $n \approx 1$ in a very wide frequency range without loss peak is a general phenomenon observed in a large number of materials.^{11,25} Thus, it is quite possible that there exist many more materials in which the dielectric relaxation is virtually not compatible with the KWW form, and the HN (or another) function will have to be used to fit the experimental data. Nevertheless, the true spectral form is of KWW type. The losses corresponding to the “universal” process are usually small, and if it coexists with another process having a distinct loss peak, it can be clearly detectable only at frequencies far away from the peak frequency. In TiBO₃, the

loss peak is comparatively narrow and the measurements in a relatively narrow frequency range made it possible to separate out the different contributions.

The mechanism suggested above can explain why in all examples mentioned in Sec. II the relaxation process compatibility with the KWW form was observed at high frequencies. The “universal” dispersion, which should be negligible at those frequencies, does not hinder the determination of the real shape of loss peak.

In conclusion, we have found that single crystals of TiBO₃ exhibit a relaxation in the frequency spectrum of dielectric permittivities, which can be described by the temperature-independent Kohlrausch-Williams-Watts (stretched exponential) type form with the superimposed low-frequency dispersion and dc component. The relaxation time was found to show a deviation from the Arrhenius law, while the spectral shape of the KWW relaxation process remains unchanged. Such a deviation is phenomenologically described and explained by the screening effects. A new formula (modified Arrhenius law) has been proposed to describe the temperature dependence of dielectric relaxation time for those materials whose relaxation process is affected by the screening effects.

ACKNOWLEDGMENT

The authors wish to thank the Natural Science and Engineering Research Council of Canada (NSERC) for support.

*Corresponding author. Email address: zye@sfu.ca

¹E. Burzo, in *Magnetic Properties of Non-Metallic Inorganic Compounds Based on Transition Elements, Boron Containing Oxides*, edited by H. P. J. Wijn, Landolt-Börnstein, New Series, Group III, Vol. 27, Pt. h (Springer-Verlag, Berlin, 1995).

²M. Eibschutz, L. Pfeiffer, and J. W. Neilsen, *J. Appl. Phys.* **41**, 1276 (1970).

³R. Diehl, W. Jantz, B. I. Nolang, and W. Wettling, *Curr. Top. Mater. Sci.* **11**, 241 (1984).

⁴B. Stahl, E. Kankeleit, R. Gellert, M. Muller, and A. Kamzin, *Phys. Rev. Lett.* **84**, 5632 (2000).

⁵Kh. G. Bogdanova, V. E. Leont'ev, and M. M. Shakirzyanov, *Phys. Solid State* **41**, 259 (1999).

⁶L. E. Svistov, V. L. Safonov, and K. R. Khachevatskaya, *Zh. Éksp. Teor. Fiz.* **112**, 564 (1997) [*JETP* **85**, 307 (1997)].

⁷L. E. Svistov and H. Benner, *Zh. Éksp. Teor. Fiz.* **115**, 1107 (1999) [*JETP* **88**, 610 (1999)].

⁸Z. Xu, R. Batchelor, F. Einstein, and Z.-G. Ye, *J. Mater. Chem.* (to be published).

⁹H. Schmid, *J. Phys. Chem. Solids* **26**, 973 (1965).

¹⁰M. Mahesh Kumar, Z. Xu, and Z.-G. Ye (unpublished).

¹¹A. K. Jonscher, *Dielectric Relaxation in Solids* (Chelsea Dielectrics, London, 1983).

¹²A. K. Jonscher, *Universal Relaxation Law* (Chelsea Dielectrics, London, 1996).

¹³S. Havriliak, Jr. and S. J. Havriliak, in *Physical Properties of Polymers Handbook*, edited by J. M. Mark (American Institute of Physics, Woodbury, NY, 1996), p. 489.

¹⁴K. Weron and A. Jurlewicz, *J. Phys. A* **26**, 395 (1993).

¹⁵P. Jund, R. Jullien, and I. Campbell, *Phys. Rev. E* **63**, 036131 (2001).

¹⁶F. Alvarez, A. Alegría, and J. Colmenero, *Phys. Rev. B* **44**, 7306 (1991); **47**, 125 (1993).

¹⁷A. Bello, E. Laredo, and M. Grimau, *Phys. Rev. B* **60**, 12 764 (1999).

¹⁸R. M. Hill, *J. Mater. Sci.* **16**, 118 (1981).

¹⁹See p. 199 of Ref. 11.

²⁰*Disorder Effects on Relaxational Processes*, edited by R. Richert and A. Blumen (Springer-Verlag, Berlin, 1994).

²¹J. Rault, *J. Non-Cryst. Solids* **271**, 177 (2000).

²²U. T. Höchli, K. Knorr, and A. Loidl, *Adv. Phys.* **39**, 405 (1990).

²³A. E. Glazounov and A. K. Tagantsev, *Appl. Phys. Lett.* **73**, 856 (1998).

²⁴G. Adam and J. H. Gibbs, *J. Chem. Phys.* **43**, 139 (1965).

²⁵A. K. Jonscher, *Nature (London)* **253**, 717 (1975).

²⁶A. A. Bokov and Z.-G. Ye, *Phys. Rev. B* (to be published).